# The Electronic Structure and Stability of the Isomers of Octamolybdate

**Adam J. Bridgeman***

*Department of Chemistry, University of Hull, Kingston-upon-Hull, United Kingdom HU6 7RX*

*Received: September 20, 2002*

The structure of the $\gamma$-, $\delta$-, $\epsilon$-, and $\xi$-isomers and the bonding in the α-, $\beta$-, $\gamma$-, $\delta$-, $\epsilon$-, and $\xi$-isomers of $[Mo_8O_{26}]^{4-}$ isopolyanions have been calculated using density functional theory. The optimized structures are in reasonably good agreement with those determined experimentally with the exception of the $\gamma$-form. For this isomer, the optimization leads to a lengthening of an internal bond, and as a result, the topology of this isomer becomes identical to that of the $\xi$-form. The electronic structure and relative stability have been probed using a bond order and valency analysis and through a decomposition of the bonding energy. The terminal Mo−O bonds possess fractional multiple bond character with similar values for those attached to four, five, and six coordinate metal atoms. The Mo−O bond order decreases as the coordination number of the oxygen increases, and a number of pseudoterminal oxygen sites have been located. The bond order analysis appears to confirm the coordination numbers of the metal atoms in the $\delta$- and $\xi$-isomers but suggests that additional contacts should be considered for one of the terminal oxygen atoms in the $\epsilon$-isomer, leading to a topology intermediate between that of the $\beta$-isomers and of the previously predicted ($\beta-\gamma$) intermediate. Despite the range of coordination numbers, charges, and bond orders, the overall bonding capacity of the oxygen atoms, measured through the full valency index, appears similar. The α- and $\delta$-isomers are predicted to be the most intrinsically stable while the $\beta$-form is the least stable. The relative stability of the isomers is due to a balance between steric interactions and favorable atomic interactions, both of which correlate with the number of Mo−O bonds. Although the α- and $\delta$-isomers possess relatively few bonds, their open structures lead to low steric crowding. The compact structure of the $\beta$-form leads to highly unfavorable steric interactions.

## Introduction

The polyoxometalates form an extremely large and diverse group of compounds with remarkable chemical and physical properties.[1,2] Polyoxometalates are used and have potential applications in a variety of fields including medicine, catalysis, solid state technology, and chemical analysis.[3,4] The polymerization of oxoanions to form extended metal−oxygen cluster anions is largely restricted to the Group 5 and 6 metals, vanadium, niobium, tantalum, molybdenum, and tungsten. These clusters, or polyoxoanions, are built primarily by edge and, occasionally, corner sharing of $MO_6$ octahedra, and the resulting cages are usually approximately spherical. Isopolyanions contain only one type of high-valent Group 5 or 6 transition metal ion, and heteropolyanions contain additional main group or transition metal cations. The primary building block is the $MO_6$ octahedron, distorted such that the metal atoms are displaced toward the vertexes that lie at the surface of the cluster. However, distorted tetrahedral $MO_4$ and trigonal bipyramidal or square pyramidal $MO_5$ units also occur. The range of cluster shapes, coordination modes, and metal ions leads to a large variety of possible structures and properties.

Isopoly and heteropolymolybdates constitute a large class of inorganic compounds. Polymeric molybdates are formed by the acidification of aqueous Mo(VI) solutions. Octamolybdate, $[Mo_8O_{26}]^{4-}$, is formed at pH values between ca. 4 and 1. The first clear evidence for isomers of octamolybdate was reported in 1970 in an infrared (IR) study by Schwing-Weill and Arnaud-Neu.[5] The most important and common isomers, α- and $\beta$-octamolybdate, can be selectively precipitated from aqueous solutions and have been structurally characterized for some time.

α-$[Mo_8O_{26}]^{4-}$ is precipitated from aqueous solutions at pH 3−4 using large organic cations. The structure of the $[(n\text{-}C_4H_9)_4N]^+$ salt was reported by Fuchs and Hartl[6] in 1976 and is shown in Figure 1. Figure 1a shows the structure in polyhedral representation. It consists of a ring of six $MO_6$ edge-shared octahedral bicapped by $MO_4$ tetrahedra leading to a structure with approximate $D_{3d}$ symmetry. As shown in the ball-and-stick representation in Figure 1b, the $MO_6$ and $MO_4$ units are distorted with short metal-oxo terminal bonds. $\beta$-$[Mo_8O_{26}]^{4-}$ is precipitated from aqueous solutions at similar pH values using small cations. The structure[7] consists of three distinct types of $MO_6$ groups. These groups are edge-shared together to form the compact structure shown in Figure 2 with approximate $C_{2h}$ symmetry. From IR and Raman studies, it appears that the $\beta$-form predominates over the α-form at pH 2 in aqueous solution.[5,8] The presence of the α-isomer in aqueous solution has been the subject of some discussion but is now established as the major component at pH 2.7 by Himeno et al. using Raman studies[8] of aqueous solution and solid state molybdates. Both isomers coexist at pH 3−4. Klemperer and Shum showed[9] that these two isomers undergo a facile isomerization in acetonitrile, with the position of the equilibrium being dependent on the countercation present. These workers also suggested a possible intramolecular mechanism for the interconversion of these disparate structures via isomeric forms, labeled $\gamma$-, ($\alpha-\gamma$), and ($\beta-\gamma$).

A third isomeric structure was first reported[10] by Niven et al. in 1991. The structure, labeled as the $\gamma$-isomer, was found to approximate the intermediate proposed by Klemperer and

* To whom correspondence should be addressed. E-mail: a.j.bridgeman@hull.ac.uk.

10.1021/jp027037l CCC: $22.00 
Published on Web 11/14/2002

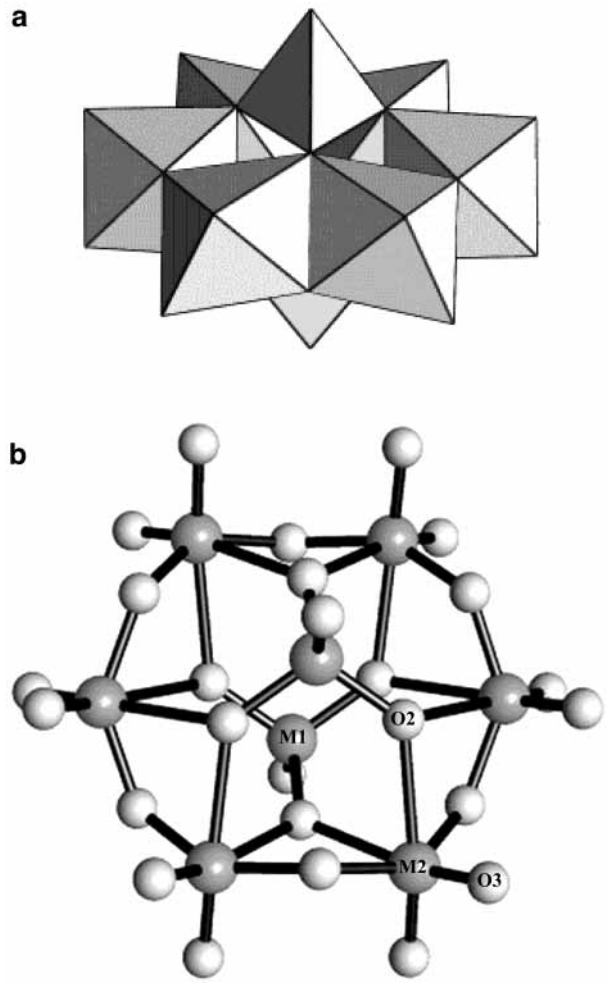


**Figure 1.** Structure of α-$[Mo_8O_{26}]^{4-}$ in (a) polyhedral and (b) ball-and-stick representation. The anion has approximate $D_{3d}$ symmetry.

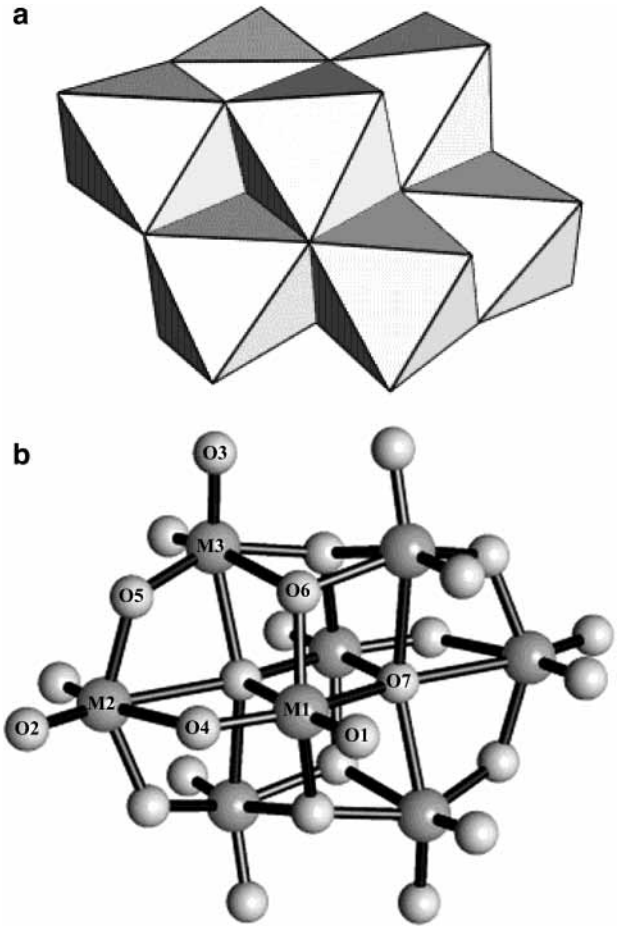


**Figure 2.** Structure of $\beta$-$[Mo_8O_{26}]^{4-}$ in (a) polyhedral and (b) ball-and-stick representation. The anion has approximate $C_{2h}$ symmetry.

Shum. This isomer, shown in Figure 3, is related to both the α- and $\beta$-forms and consists of an edge-shared arrangement of six $MO_6$ octahedra and two $MO_5$ square pyramids. Himeno et al. have reported[8] the IR and Raman spectra of the $\gamma$-form in the solid state but found no evidence that it exists in aqueous solution in appreciable amounts.

More recently, Zubieta and co-workers,[11−13] Xi et al.[14] and Xu et al.[15] have reported the structures of three further isomers in the solid state using a variety of organic or metal-based cations to direct the microstructure of the polyoxometalate. The $\delta$-isomer,[11,13,14] shown in Figure 4, is constructed from four $MO_6$ octahedra and four $MO_4$ tetrahedra. The structure consists of a $M_6O_6$ ring made from two pairs of edge-shared octahedra linked by corner sharing with two tetrahedra. As in the α-form, the ring is bicapped by tetrahedra. The $\epsilon$-isomer,[11] shown in Figure 5, consists of a ring of six $MO_5$ square pyramids and two $MO_6$ octahedra linked via edge sharing. The structure is unusual among the octamolybdate isomers, and fairly unique in the molybdates, in having an apparently very open structure. A sixth isomer,[15] labeled as the $\xi$-form, consists of four $MO_6$ octahedra and four $MO_5$ units. The structure, shown in Figure 6, contains a ring of four octahedra and two distorted trigonal bipyramids, linked by corner and edge sharing, bicapped by two square pyramids. The $\gamma$-, $\delta$-, $\epsilon$-, and $\xi$-isomers have only $C_i$ symmetry in the solid state.

As can be seen from Figures 1−6, the various isomeric forms of octamolybdate may be, at least conceptually, interconverted by fairly small bond elongations and compressions and by rotation of the polyhedra.

Although the synthesis, structural and spectroscopic analysis, and development of applications of polyoxoanions are extremely rich areas of research, relatively few high-level computational studies have been reported—reflecting the intensive computational demands imposed by the large size of these species. Most of the first principle studies related to polyoxoanions have been carried out by Poblet, Bénard, and co-workers,[16−27] at the Hartree−Fock (HF) and density functional (DF) levels of theory and by Bridgeman and Cavigliasso[28−37] and Borshch and co-workers[38−40] at the DF level. These studies include a number related to the Keggin anions.[24−27,36] We have recently completed a detailed study[35] of the electronic structure of α- and $\beta$-$[Mo_8O_{26}]^{4-}$ at the DF level. That study included a comparison of the optimized structures of the ions, treated as pseudo-gas phase species, with the crystallographically determined geometries and their bonding and stability. Particular emphasis was placed on the detection of molecular orbital "closed loops" formed by the metal centers and the bridging oxygen atoms linking the octahedral units. The number of such loops per $MO_6$ unit has been proposed by Nomiya and Miwa[41] as a measure of the relative stability of polyanion cages. Closed loops with both $\sigma$- and $\pi$-bonding characteristics were identified, but no connection with the stability of these isomers could be identified. However, a combined analysis of the bond orders and valency and the bonding energetics was found to provide useful insights into the origin of the relative stabilities in terms of the strength of the bonding and the packing. In this paper, this work is extended to the lower symmetry $\gamma$-, $\delta$-, $\epsilon$-, and $\xi$-isomers and

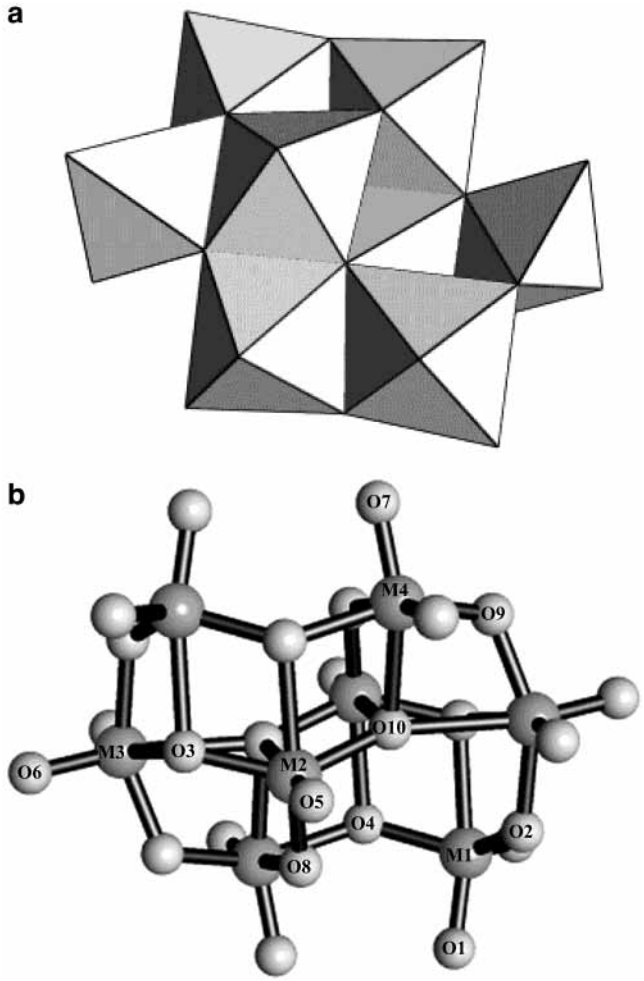


**Figure 3.** Structure of $\gamma$-$[Mo_8O_{26}]^{4-}$ in (a) polyhedral and (b) ball-and-stick representation. The anion has $C_i$ symmetry.

the structural stability and bonding in the full set of presently known octamolybdates are compared.

## Computational Approach

All DF calculations reported in this work were performed with the ADF 2000.02 program.[42,43] Functionals based on the Vosko−Wilk−Nusair (VWN)[44] form of the local density approximation (LDA),[45] and on a combination (labeled BP86) of Becke's 1988 exchange[46] and Perdew's 1986 correlation[47] corrections to the LDA, and Slater type orbital (STO) basis sets of triple-$\zeta$ quality incorporating frozen cores and the ZORA relativistic approach (ADF O.1s and Mo.3d type IV) were utilized. These basis sets combined with the VWN functional have been shown in tests[28,29,37] on several $MO_4$, $M_2O_7$, and $M_6O_{19}$ species to yield better agreement with experimental geometries and vibrational frequencies than gradient-corrected functionals using STO basis sets and VWN, gradient-corrected, and hybrid functionals with available Gaussian type orbital (GTO) basis sets when computationally modeled as gas phase species. Hence, all geometry optimizations reported here have been carried out using LDA methods. Date on thermochemistry and bonding energetics have been obtained using single point BP86 calculations to compensate for the overbinding associated with the LDA method. Bond and valency indexes were obtained according to the definitions proposed by Mayer[48] and by Evarestov and Veryazov,[49] respectively, using a program[50] designed for the calculation from the ADF output.

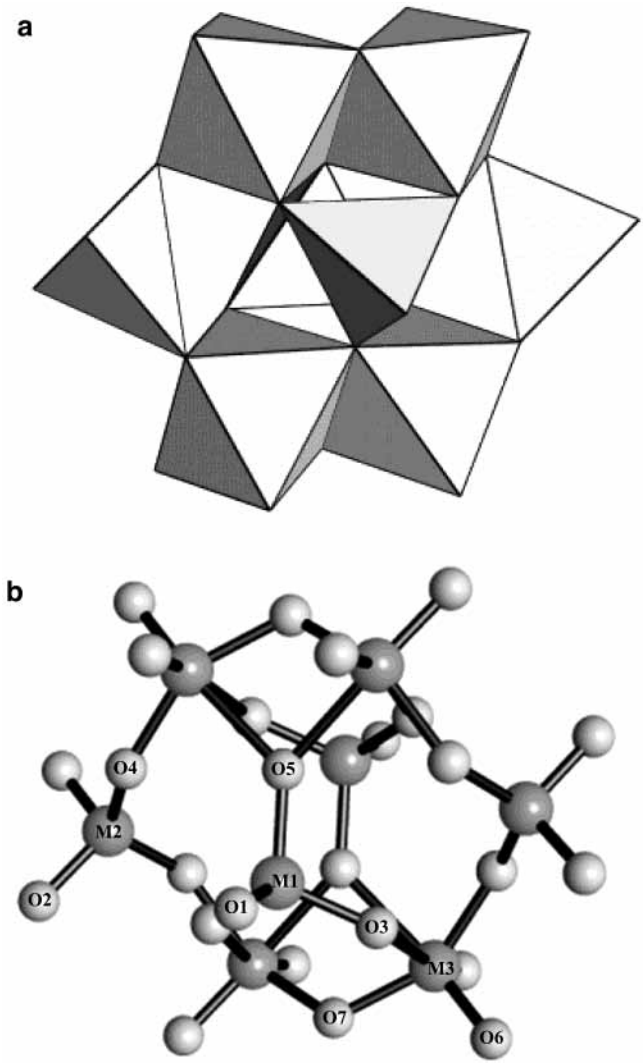


**Figure 4.** Structure of $\delta$-$[Mo_8O_{26}]^{4-}$ in (a) polyhedral and (b) ball-and-stick representation. The anion has approximate $C_{2h}$ symmetry.

## Results and Discussion

**Molecular Structures.** The structures and atom number scheme for $\alpha$-, $\beta$-, $\gamma$-, $\delta$-, $\epsilon$-, and $\xi$-$[Mo_8O_{26}]^{4-}$ are shown in Figures 1−6. The optimized structures are given in Tables 1−6, together with a comparison with the crystallographically determined bond lengths.

As outlined above, the $\alpha$-form consists of a ring of six $MO_6$ units bicapped by two $MO_4$ groups. The four coordinate Mo ($Mo_{4c}$, M1) atoms are bonded to one terminal oxo ($O_t$, O1) and three $\mu_3$ ($O_{3c}$, O2) oxygen atoms, which link the tetrahedra to the octahedra. The six coordinate Mo ($Mo_{6c}$, M2) atoms are bonded to two terminal oxo ($O_t$, O3), two $\mu_2$ ($O_{2c}$, O4), which link the octahedra and two $\mu_3$ ($O_{3c}$, O2) oxygen atoms. As detailed elsewhere[35] and shown in Table 1, the agreement between the calculated and the experimental geometries is very good. Although the crystallographically determined structure[6] has only $C_i$ symmetry, the averaged structural parameters[51] and the optimization lead to a structure with $D_{3d}$ symmetry.

The structure of the $\beta$-form is made from three types of $MO_6$ units, containing metal atoms labeled M1, M2, and M3. As shown in Figure 2 and Table 2, the structure is more compact than that of the $\alpha$-isomer. The oxygen atoms fall broadly into four categories, terminal ($O_t$: O1, O2, and O3), $\mu_2$ ($O_{2c}$: O4, O5), $\mu_3$ ($O_{3c}$: O6), and $\mu_5$ ($O_{5c}$, O7) oxygen. The O4 atoms are also formally of the $\mu_2$ type, but as can be seen in Table 2, the

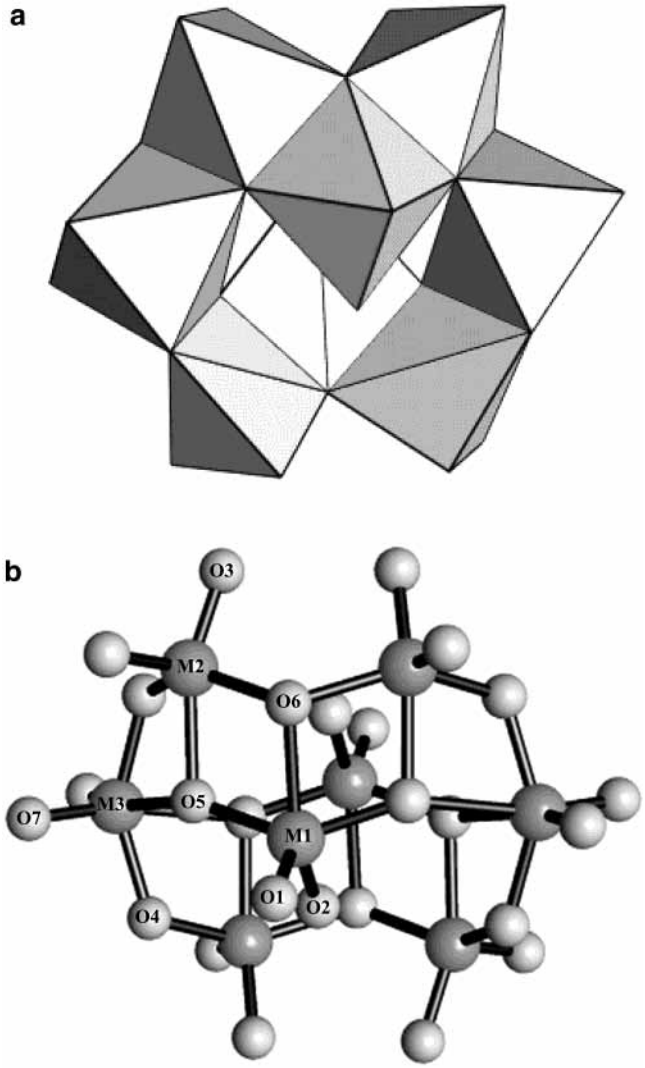


**Figure 5.** Structure of $\epsilon$-$[Mo_8O_{26}]^{4-}$ in (a) polyhedral and (b) ball-and-stick representation. The anion has approximate $C_{2h}$ symmetry.

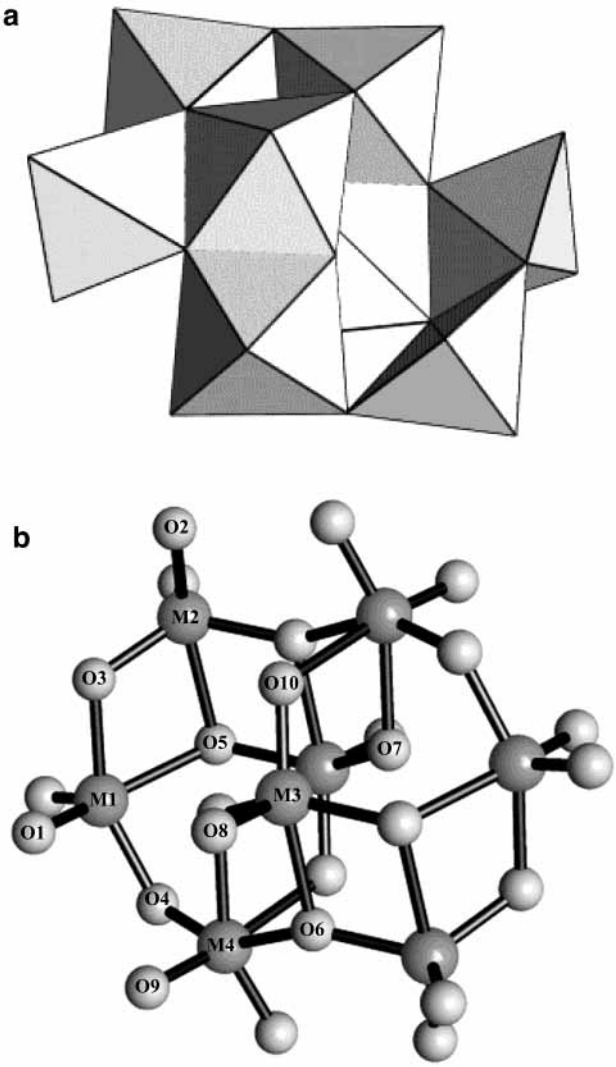


**Figure 6.** Structure of $\xi$-$[Mo_8O_{26}]^{4-}$ in (a) polyhedral and (b) ball-and-stick representation. The anion has $C_i$ symmetry.

M1−O4 and M2−O4 bonds are more typical of terminal Mo−O and high-coordinate sites, respectively. The O4 sites have therefore been classified[51] as pseudoterminal ($O_{pt}$). As detailed elsewhere,[35] the agreement between the calculated and the experimental structures is good except for the longest Mo−O bonds (M2−O4, M1−O7, and M2−O7) for which the calculation underestimates the bond length by up to 10 pm.

The crystallographically determined[10] structure of the $\gamma$-isomer consists of a $M_6O_6$ ring bicapped by two $MO_6$ groups. The ring is made from two pairs of edge-shared $MO_6$ groups (M = $M_{6c}$: M3 and M4) linked together by corner sharing to two $MO_5$ groups (M = $M_{5c}$: M1). The $M_{5c}$ atoms are bonded to two terminal ($O_t$: O1), one $\mu_2$ ($O_{2c}$: O2), and two $\mu_3$ ($O_{3c}$: O3 and O4) oxygen atoms. The M3 atoms are bonded to two terminal ($O_t$: O6), two $\mu_2$ ($O_{2c}$: O2 and O9), one $\mu_3$ ($O_{3c}$: O3), and one $\mu_4$ ($O_{4c}$: O10) oxygen atoms. The M3 atoms are also bonded to two terminal ($O_t$: O7), two $\mu_2$ ($O_{2c}$: O8 and O9), one $\mu_3$ ($O_{3c}$: O4), and one $\mu_4$ ($O_{4c}$: O10) oxygen atoms. Although the coordination is similar, the details of the bonding around M3 and M4 are quite different, as detailed below. The O8 atoms are labeled as $\mu_2$, but as can be seen in Table 3, the M2−O8 and M3−O8 bonds are more typical of terminal Mo−O and high-coordinate sites, respectively. The O8 sites, therefore, may be classified as pseudoterminal ($O_{pt}$). The ring is capped by two $MO_6$ groups (M = $M_{6c}$: M2). The coordination around the M2 atoms consists of one terminal ($O_t$: O5), one $\mu_2$ ($O_{2c}$: O2), two $\mu_3$ ($O_{3c}$: O3 and O4), and one $\mu_4$ ($O_{4c}$: O10) oxygen atoms.

**TABLE 1: Calculated and Experimental[51] Bond Distances and Bond Orders for the Optimized and Experimental Structure of α-$[Mo_8O_{26}]^{4-}$[a]**

| tetrahedral sites | | | | | | | |
|---|---|---|---|---|---|---|---|
| | | bond length (Å) | | | | | |
| type | | expt | calcd | type | | bond order | |
| $Mo_{4c}-O_t$ | M1−O1 | 1.71 | 1.74 | $Mo_{4c}-O_t$ | M1−O1 | 1.57 | 1.50 |
| $Mo_{4c}-O_{3c}$ | M1−O2 | 1.78 | 1.80 | $Mo_{4c}-O_{3c}$ | M1−O2 | 1.01 | 0.97 |
| **octahedral sites** | | | | | | | |
| | | bond length (Å) | | | | | |
| type | | expt | calcd | type | | bond order | |
| $Mo_{6c}-O_t$ | M2−O3 | 1.69 | 1.72 | $Mo_{6c}-O_t$ | M2−O3 | 1.59 | 1.65 |
| $Mo_{6c}-O_{2c}$ | M2−O4 | 1.91 | 1.92 | $Mo_{6c}-O_{2c}$ | M2−O4 | 0.65 | 0.68 |
| $Mo_{6c}-O_{3c}$ | M2−O2 | 2.44 | 2.40 | $Mo_{6c}-O_{3c}$ | M2−O2 | 0.16 | 0.19 |

[a] The atom numbering is defined in Figure 1b. The experimental bond lengths and orders are mean values for the various bond types assuming $D_{3d}$ symmetry.

As shown in Table 3, the agreement between the calculated and the experimental bond lengths is much poorer for the

**TABLE 2: Calculated and Experimental[51] Bond Distances and Bond Orders for the Optimized and Experimental Structure of $\beta$-$[Mo_8O_{26}]^{4-a}$**

| octahedral sites | | | | | | | |
|---|---|---|---|---|---|---|---|
| | | bond length (Å) | | | | | |
| type | | expt | calcd | type | | bond order | |
| $Mo-O_t$ | M1−O1 | 1.70 | 1.72 | $Mo-O_t$ | M1−O1 | 1.61 | 1.61 |
| | M2−O2 | 1.70 | 1.74 | | M2−O2 | 1.58 | 1.58 |
| | M3−O3 | 1.70 | 1.73 | | M3−O3 | 1.59 | 1.60 |
| $Mo-O_{2c}$ | M1−O4 | 1.75 | 1.78 | $Mo-O_{2c}$ | M1−O4 | 1.25 | 1.21 |
| | M2−O4 | 2.29 | 2.20 | | M2−O4 | 0.24 | 0.27 |
| | M2−O5 | 1.93 | 1.92 | | M2−O5 | 0.65 | 0.66 |
| | M3−O5 | 1.89 | 1.91 | | M3−O5 | 0.67 | 0.67 |
| $Mo-O_{3c}$ | M1−O6 | 1.95 | 1.96 | $Mo-O_{3c}$ | M1−O6 | 0.57 | 0.54 |
| | M3−O6 | 2.00 | 1.98 | | M3−O6 | 0.49 | 0.51 |
| | M3−O6 | 2.35 | 2.35 | | M3−O6 | 0.22 | 0.22 |
| $Mo-O_{5c}$ | M1−O7 | 2.15 | 2.08 | $Mo-O_{5c}$ | M1−O7 | 0.32 | 0.39 |
| | M1−O7′ | 2.38 | 2.38 | | M1−O7′ | 0.22 | 0.21 |
| | M2−O7 | 2.45 | 2.56 | | M2−O7 | 0.21 | 0.16 |
| | M3−O7 | 2.32 | 2.35 | | M3−O7 | 0.23 | 0.23 |

[a] The atom numbering is defined in Figure 2b. The experimental bond lengths and orders are mean values for the various bond types assuming $C_{2h}$ symmetry.

**TABLE 3: Calculated and Experimental[10] Bond Distances and Bond Orders for the Optimized and Experimental Structure of $\gamma$-$[Mo_8O_{26}]^{4-a}$**

| square pyramidal sites | | | | | | | |
|---|---|---|---|---|---|---|---|
| | | bond length (Å) | | | | | |
| type | | expt | calcd | type | | bond order | |
| $Mo_{5c}-O_t$ | M1−O1 | 1.70 | 1.73 | $Mo_{5c}-O_t$ | M1−O1 | 1.55 | 1.58 |
| $Mo_{5c}-O_{2c}$ | M1−O2 | 1.83 | 1.89 | $Mo_{5c}-O_{2c}$ | M1−O2 | 0.83 | 0.76 |
| $Mo_{5c}-O_{3c}$ | M1−O3 | 1.89 | 1.94 | $Mo_{5c}-O_{3c}$ | M1−O3 | 0.62 | 0.61 |
| | M1−O4 | 2.35 | 2.18 | | M1−O4 | 0.21 | 0.29 |
| octahedral sites | | | | | | | |
| | | bond length (Å) | | | | | |
| type | | expt | calcd | type | | bond order | |
| $Mo_{6c}-O_t$ | M2−O5 | 1.69 | 1.72 | $Mo_{6c}-O_t$ | M2−O5 | 1.57 | 1.60 |
| | M3−O6 | 1.70 | 1.73 | | M3−O6 | 1.57 | 1.58 |
| | M4−O7 | 1.70 | 1.73 | | M4−O7 | 1.61 | 1.62 |
| $Mo_{6c}-O_{2c}$ | M2−O8 | 1.75 | 1.77 | $Mo_{6c}-O_{2c}$ | M2−O8 | 1.29 | 1.25 |
| | M3−O2 | 1.99 | 1.97 | | M3−O2 | 0.50 | 0.62 |
| | M3−O9 | 1.93 | 1.90 | | M3−O9 | 0.68 | 0.73 |
| | M4−O8 | 2.37 | 2.24 | | M4−O8 | 0.22 | 0.24 |
| | M4−O9 | 1.90 | 1.92 | | M4−O9 | 0.69 | 0.63 |
| $Mo_{6c}-O_{3c}$ | M2−O3 | 2.29 | 2.21 | $Mo_{6c}-O_{3c}$ | M2−O3 | 0.16 | 0.20 |
| | M2−O4 | 1.88 | 1.94 | | M2−O4 | 0.71 | 0.52 |
| | M3−O3 | 2.15 | 2.07 | | M3−O3 | 0.30 | 0.34 |
| | M4−O4 | 2.01 | 2.11 | | M4−O4 | 0.37 | 0.37 |
| $Mo_{6c}-O_{4c}$ | M2−O10 | 2.49 | 2.40 | $Mo_{6c}-O_{4c}$ | M2−O10 | 0.15 | 0.18 |
| | M2−O10′ | 1.91 | 1.87 | | M2−O10′ | 0.63 | 0.75 |
| | M3−O10 | 2.49 | 3.06 | | M3−O10 | 0.17 | 0.06 |
| | M4−O10 | 2.21 | 2.18 | | M4−O10 | 0.25 | 0.28 |

[a] The atom numbering is defined in Figure 3b. The experimental bond lengths and orders are mean values for the various bond types.

$\gamma$-isomer than for the $\alpha$- and $\beta$-forms and indeed for the other isomers detailed below. The largest discrepancies involve the coordination around the formally six coordinate M3 atoms. The M3−O10 bond is located trans to a short and presumably strong $Mo-O_t$ group. This bond lengthens from 2.49 Å to over 3 Å so that M3 becomes effectively five coordinate with a distorted square pyramidal coordination. Associated with this decrease in the bonding interaction between O10 and M3 is significant shortening of the M4−O10, M2−O10, M3−O2, and M3−O9 bonds.

The $\gamma$-isomer is precipitated from aqueous solution at pH 6, much higher than that required for either the $\alpha$- or the $\beta$-forms, using a large cation. As noted above, Himeno et al. could not find[8] any evidence for its existence in aqueous solution. It appears then that this isomer is unlikely to represent a thermodynamically stable species in solution and that it requires specific coordination through H-bonding to be stabilized. The rearrangement suggested by the optimization involves only the lengthening of any already long, and presumably weak, bond with only slight compensating movements of other atoms. The isomeric form produced by the optimization strongly resembles that produced by the optimization of the $\xi$-form, and it appears that these two isomers are closely linked.

The structure of the $\delta$-isomer also consists of a $M_6O_6$ ring bicapped by $MO_4$ tetrahedra. The ring is made from two pairs of edge-linked $MO_6$ groups ($M = M_{6c}$: M3) linked together by corner sharing to two $MO_4$ groups ($M = M_{4c}$: M2). The $M_{6c}$ atoms are bonded to two terminal ($O_t$: O6), three $\mu_2$ ($O_{2c}$: O3, O4, and O7), and one $\mu_3$ ($O_{3c}$: O5) oxygen atoms. The M3 atoms are bonded to two terminal ($O_t$: O2) and two $\mu_2$ ($O_{2c}$: O4) oxygen atoms. The ring is bicapped by $MO_4$ ($M = M_{4c}$: M1) groups consisting of one terminal ($O_t$: O2), two $\mu_2$ ($O_{3c}$: O4), and one $\mu_3$ ($O_{3c}$: O5) oxygen atoms ($M = M_{6c}$: M2). Although there are some small differences in the details of the reported structures of the $\delta$-isomer,[13] the calculated structure is in good agreement with the crystal structure, as shown in Table 4. Although formally of $C_i$ symmetry, the averaged structural parameters and the optimization lead to a structure with $C_{2h}$ symmetry. Also noticeable in the crystal structure is a reasonably close contact, at ca. 2.9 Å, between the $Mo_{4c}$ (M1) atoms in the $MO_4$ caps and the formally $\mu_3$ oxygen atoms (O5′). No marked decrease in this bond length is observed upon optimization. Further clarification on the coordination number of M1 is gained through the bond order analysis presented below.

The $\epsilon$-isomer consists of a $M_6O_6$ ring bicapped by two $MO_5$ groups. The ring is made from two pairs of corner-linked $MO_5$ groups ($M = M_{5c}$: M2) linked together by edge sharing to two $MO_6$ groups ($M = M_{6c}$: M3). The M2 atoms are bonded to two terminal ($O_t$: O2), one $\mu_2$ ($O_{2c}$: O4), and two $\mu_3$ ($O_{3c}$: O5 and O6) oxygen atoms. The $M_{6c}$ atoms are bonded to two terminal ($O_t$: O7), two $\mu_2$ ($O_{2c}$: O4), and two $\mu_3$ ($O_{3c}$: O5) oxygen atoms. The capping groups consist of $MO_5$ units ($M = M_{5c}$: M1 atoms). The M1 atoms are bonded to two terminal ($O_t$: O1 and O2) and three $\mu_3$ ($O_{3c}$: O5 and O6) oxygen atoms. The calculated bond lengths, listed in Table 5, are, again, in good agreement with those determined experimentally. Although formally of $C_i$ symmetry, the averaged structural parameters and the optimization lead to a structure with $C_{2h}$ symmetry. The $\epsilon$-isomer has been described[12] as an open structure with a central cavity presumably due to the mode of attachment of the bicapping groups. However, it is noticeable in the crystal structure that there are close contacts between one of the terminal oxygen atoms (O2) on the $MO_5$ ($M = M1$) caps and the metal atoms in the $MO_5$ groups in the ring ($M = M2$) and on the other cap ($M = M1'$) of 2.72 and 2.90 Å, respectively. These bond lengths decrease somewhat to 2.61 and 2.73 Å, respectively, upon optimization. Further clarification on this matter is gained through the bond order analysis presented below.

The $\xi$-isomer also consists of a $M_6O_6$ ring bicapped by two $MO_6$ octahedra. The ring is made from two pairs of edge-linked $MO_5$ groups ($M = M_{5c}$: M1 and M2) linked together by corner sharing to two $MO_6$ octahedra ($M = M_{6c}$: $M = M4$). The M1 atoms are bonded to two terminal ($O_t$: O1), two $\mu_2$ ($O_{2c}$: O3

**TABLE 4: Calculated and Experimental[11] Bond Distances and Bond Orders for the Optimized and Experimental Structure of $\delta$-$[Mo_8O_{26}]^{4-a}$**

| tetrahedral sites | | | | | | | |
|---|---|---|---|---|---|---|---|
| | | bond length (Å) | | | | | |
| type | | expt | calcd | type | | bond order | |
| $Mo_{4c}-O_t$ | M1−O1 | 1.70 | 1.73 | $Mo_{4c}-O_t$ | M1−O1 | 1.53 | 1.56 |
| | M2−O2 | 1.70 | 1.73 | | M2−O2 | 1.54 | 1.55 |
| $Mo_{4c}-O_{2c}$ | M1−O3 | 1.77 | 1.78 | $Mo_{4c}-O_{2c}$ | M1−O3 | 1.06 | 1.01 |
| | M2−O4 | 1.83 | 1.84 | | M2−O4 | 0.76 | 0.79 |
| $Mo_{4c}-O_{3c}$ | M1−O5 | 1.84 | 1.84 | $Mo_{4c}-O_{3c}$ | M1−O5 | 0.76 | 0.79 |
| | (M1−O5′ | 2.89 | 2.81) | | (M1−O5 | 0.06 | 0.08) |
| octahedral sites | | | | | | | |
| | | bond length (Å) | | | | | |
| type | | expt | calcd | type | | bond order | |
| $Mo_{6c}-O_t$ | M3−O6 | 1.70 | 1.73 | $Mo_{6c}-O_t$ | M3−O6 | 1.60 | 1.62 |
| $Mo_{6c}-O_{2c}$ | M3−O3 | 2.31 | 2.25 | $Mo_{6c}-O_{2c}$ | M3−O3 | 0.21 | 0.22 |
| | M3−O4 | 1.95 | 1.97 | | M3−O4 | 0.50 | 0.49 |
| | M3−O7 | 1.91 | 1.92 | | M3−O7 | 0.67 | 0.69 |
| $Mo_{6c}-O_{3c}$ | M3−O5 | 2.34 | 2.35 | $Mo_{6c}-O_{3c}$ | M3−O5 | 0.18 | 0.17 |

[a] The atom numbering is defined in Figure 4b. The experimental bond lengths and orders are mean values for the various bond types assuming $C_{2h}$ symmetry.

**TABLE 5: Calculated and Experimental[11] Bond Distances and Bond Orders for the Optimized and Experimental Structure of $\epsilon$-$[Mo_8O_{26}]^{4-a}$**

| square pyramidal sites | | | | | | | |
|---|---|---|---|---|---|---|---|
| | | bond length (Å) | | | | | |
| type | | expt | calcd | type | | bond order | |
| $Mo_{5c}-O_t$ | M1−O1 | 1.68 | 1.72 | $Mo_{5c}-O_t$ | M1−O1 | 1.52 | 1.55 |
| | M1−O2 | 1.75 | 1.77 | | M1-O2 | 1.16 | 1.07 |
| | M2−O3 | 1.71 | 1.72 | | M2−O3 | 1.58 | 1.59 |
| $Mo_{5c}-O_{2c}$ | M2−O4 | 1.90 | 1.89 | $Mo_{5c}-O_{2c}$ | M2-O4 | 0.73 | 0.74 |
| $Mo_{5c}-O_{3c}$ | M1−O5 | 1.87 | 1.87 | $Mo_{5c}-O_{3c}$ | M1−O5 | 0.71 | 0.72 |
| | M1−O6 | 2.21 | 2.24 | | M1−O6 | 0.27 | 0.29 |
| | M2−O5 | 2.11 | 2.13 | | M2−O5 | 0.30 | 0.27 |
| | M2−O6 | 2.06 | 2.01 | | M2−O6 | 0.46 | 0.47 |
| | (M1′−O2 | 2.90 | 2.73) | | (M1′−O2 | 0.12 | 0.16) |
| | (M2−O2 | 2.72 | 2.61) | | (M2−O2 | 0.19 | 0.12) |
| octahedral sites | | | | | | | |
| | | bond length (Å) | | | | | |
| type | | expt | calcd | type | | bond order | |
| $Mo_{6c}-O_t$ | M3−O7 | 1.69 | 1.72 | $Mo_{6c}-O_t$ | M3−O6 | 1.58 | 1.60 |
| $Mo_{6c}-O_{2c}$ | M3−O4 | 1.94 | 1.94 | $Mo_{6c}-O_{2c}$ | M3−O3 | 0.64 | 0.61 |
| $Mo_{6c}-O_{3c}$ | M3−O5 | 2.35 | 2.28 | $Mo_{6c}-O_{3c}$ | M3−O4 | 0.18 | 0.19 |

[a] The atom numbering is defined in Figure 5b. The experimental bond lengths and orders are mean values for the various bond types assuming $C_{2h}$ symmetry.

and O4), and one $\mu_3$ ($O_{3c}$: O5) oxygen atoms. The M2 atoms are bonded to two terminal ($O_t$: O2), one $\mu_2$ ($O_{2c}$: O3), and two $\mu_3$ ($O_{3c}$: O5 and O6) oxygen atoms. The M2 atoms are bonded to two terminal ($O_t$: O1), two $\mu_2$ ($O_{2c}$: O3 and O4), and one $\mu_3$ ($O_{3c}$: O5) oxygen atoms. The M4 atoms are bonded to two terminal ($O_t$: O9), two $\mu_2$ ($O_{2c}$: O4 and O10), and two $\mu_3$ ($O_{3c}$: O6 and O7) oxygen atoms. The O10 atoms are labeled as $\mu_2$, but as can be seen in Table 6, the M3−O10 and M4−O10 bonds are actually more typical of terminal Mo−O and high-coordinate sites, respectively, and the O10 atom may be classified as pseudoterminal ($O_{pt}$). The ring is capped by two $MO_6$ groups (M = $M_{6c}$: M3). The M3 atoms are bonded to one terminal ($O_t$: O8), one $\mu_2$ ($O_{2c}$: O10), and four $\mu_3$ ($O_{3c}$:

**TABLE 6: Calculated and Experimental[15] Bond Distances and Bond Orders for the Optimized and Experimental Structure of $\xi$-$[Mo_8O_{26}]^{4-a}$**

| square pyramidal sites | | | | | | | |
|---|---|---|---|---|---|---|---|
| | | bond length (Å) | | | | | |
| type | | expt | calcd | type | | bond order | |
| $Mo_{5c}-O_t$ | M1−O1 | 1.69 | 1.72 | $Mo_{5c}-O_t$ | M1−O1 | 1.60 | 1.59 |
| | M2−O2 | 1.71 | 1.73 | | M2−O2 | 1.61 | 1.61 |
| $Mo_{5c}-O_{2c}$ | M1−O3 | 2.02 | 2.00 | $Mo_{5c}-O_{2c}$ | M1−O3 | 0.53 | 0.54 |
| | M1−O4 | 1.94 | 1.91 | | M1−O4 | 0.67 | 0.70 |
| | M2−O3 | 1.83 | 1.86 | | M2−O3 | 0.81 | 0.82 |
| $Mo_{5c}-O_{3c}$ | M1−O5 | 2.18 | 2.12 | $Mo_{5c}-O_{3c}$ | M1−O5 | 0.29 | 0.34 |
| | M2−O5 | 2.24 | 2.30 | | M2−O5 | 0.24 | 0.23 |
| | M2−O6 | 1.89 | 1.91 | | M2−O6 | 0.60 | 0.62 |
| | (M1−O7 | 2.53 | 2.70) | | (M1−O7 | 0.17 | 0.12) |
| octahedral sites | | | | | | | |
| | | bond length (Å) | | | | | |
| type | | expt | calcd | type | | bond order | |
| $Mo_{6c}-O_t$ | M3−O8 | 1.69 | 1.72 | $Mo_{6c}-O_t$ | M3−O8 | 1.57 | 1.60 |
| | M4−O9 | 1.73 | 1.73 | | M4−O9 | 1.61 | 1.61 |
| $Mo_{6c}-O_{2c}$ | M3−O10 | 1.73 | 1.77 | $Mo_{6c}-O_{2c}$ | M3−O10 | 1.30 | 1.27 |
| | M4−O4 | 1.88 | 1.91 | | M4−O4 | 0.69 | 0.66 |
| | M4−O10 | 2.34 | 2.28 | | M4−O10 | 0.21 | 0.23 |
| $Mo_{6c}-O_{3c}$ | M3−O5 | 1.89 | 1.92 | $Mo_{6c}-O_{3c}$ | M3−O5 | 0.66 | 0.64 |
| | M3−O6 | 2.20 | 2.25 | | M3−O6 | 0.20 | 0.18 |
| | M3−O7 | 1.92 | 1.90 | | M3−O7 | 0.62 | 0.69 |
| | M3−O7′ | 2.53 | 2.42 | | M3−O7′ | 0.15 | 0.17 |
| | M4−O6 | 2.03 | 2.03 | | M4−O6 | 0.34 | 0.36 |
| | M4−O7 | 2.14 | 2.21 | | M4−O7 | 0.27 | 0.25 |

[a] The atom numbering is defined in Figure 6b. The experimental bond lengths and orders are mean values for the various bond types.

O5, O6, O7, and O7′) oxygen atoms. The agreement between the calculated and the experimental structures, shown in Table 6, is good except for the longest Mo−O bonds (M2−O5, M3−O7′, and M4−O10) for which the calculation underestimates the bond length by up to 10 pm. Although M1 has been considered[15] five coordinate, it is noticeable that there is a close contact with the $\mu_3$ O7 atom at 2.53 Å. This bond lengthens to 2.70 Å in the optimized structure. As outlined above, this coordinate controls the distinction between the $\gamma$- and the $\xi$-isomers. The ring in the $\gamma$- and $\xi$-isomer has been considered[10,15] to be composed of four $MO_6$ and two $MO_5$ groups and two $MO_6$ and four $MO_5$ groups, respectively. If the M1−O7 contact in the $\xi$-isomer is considered a bond or if the M3−O10 contact in the $\gamma$-isomer is not considered a bond, then the topology of the isomers is the same. Further clarification on this matter is gained through the bond order analysis presented below.

**Bond Order and Valency.** Mayer bond order indexes are given alongside the structural parameters in Tables 1−6 for the isomers in their crystallographically determined (expt) and LDA-optimized (calcd) structures. Although Mayer bond orders are known to be basis-set dependent,[52] they are a powerful tool for describing localized bonding when a consistent basis set is employed. Figure 7 shows the variation in the bond order with bond length for all of the 164 Mo−O bonds studied. The variation is well-described by an exponential decay with bond length of the type suggested by Pauling.[53] Also included on the figure is the relationship deduced by Tytko et al.[51] using a classical bond valence approach. The two approaches agree reasonably well for the shortest and longest bonds, those involving terminal and pseudoterminal and multiply bridging oxygen atoms, respectively. Deviations of ca. 0.3 units are observed in the intermediate distance range typified by bonds

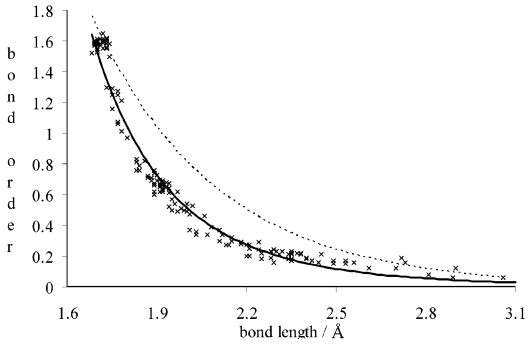


**Figure 7.** Variation of bond order with bond length for the isomers of octamolybdate. The broken line corresponds to the classical valence approach.[51]

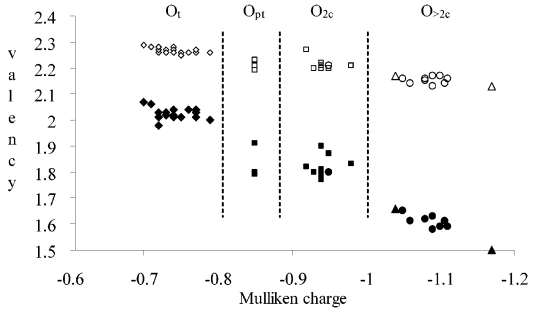


**Figure 8.** Variation of oxygen covalency (shaded) and full valency (open) with Mulliken charge for the isomers of octamolybdate. The oxygen atoms are labeled by their coordination numbers as terminal (diamonds), $\mu_2$ (squares), $\mu_3$ (circles), and $\{\mu_4, \mu_5\}$ (triangles).

involving $\mu_2$ oxygen. The classical bond valence approach is predicated on such bonds having a bond order of unity to satisfy oxygen's divalency requirement. The Mayer values for such bonds, however, are a measure of two-center covalency and deviate from unity due to the inherent electrovalent character of the Mo−O bond.

The terminal bonds exhibit significant multiple bond character with bond orders of ca. 1.5 for Mo−$O_t$ bonds in tetrahedral, square pyramidal, and octahedral sites. The index is appreciably smaller than the maximum possible covalency[31] due to the importance of ionic contributions to the bonding as described in more detail below. The Mayer analysis also enables the nature of the bonding to pseudoterminal ($O_{pt}$) oxygen atoms in the polyoxoanions to be established. As described above, the O4, O8, and O10 sites in the $\beta$-, $\gamma$-, and $\xi$-isomers, respectively, are labeled as $\mu_2$ but actually are involved in one short and one long bond. The bond orders for these interactions are predicted to be ca. 1.25 and 0.25 for the short and long bonds, respectively. The bond order for the short Mo−$O_{pt}$ bond is around twice as large as that for a true Mo−$O_{2c}$ interaction and around three-fourths of that of a true Mo−$O_t$ bond. The bond order for the long Mo−$O_{pt}$ bonds is typical of that for a high coordinate oxygen. Although characterized by fairly small bond orders, these long interactions must be considered as genuine covalent interactions.

As detailed above, the optimized structure for the $\gamma$-isomer leads to a considerably longer M3−O10 bond than observed crystallographically. The M3−O10 bond order similarly reduces from 0.17 in the experimental structure to 0.06 in the optimized structure. Bond orders of this size are typical of those between atoms that would not normally be considered as bonded in a classical approach such as the oxygen atoms of the polyoxoanions. As suggested above, it appears that the optimization reduces the tension in the structure induced by the crystal environment by reducing the coordination number from six to five for M3 in this isomer and this leads to a topology equivalent to that of the $\xi$-form. The analogous contact in the structure of $\xi$-isomer occurs between the formally five coordinate M1 atom and O7. This bond lengthens considerably in the optimization with a significant decrease in the bond order.

The M1 atoms in the tetrahedral caps of the $\delta$-isomer are in reasonably close contact with the O5 atoms located on the other cap. Such an interaction would lead to an isomer with similar topology to the ($\alpha-\gamma$) isomer suggested as an intermediate by Klemperer and Shum.[9] The geometry optimization, however, does not lead to any significant reduction in the bond length, and the bond order for this interaction is again too small to be considered significant. M1 appears genuinely to be four coordinate, and this is not enforced by the crystal environment.

Close contacts are also observed in the structure of the $\epsilon$-isomer, particularly, as noted above, between one of the terminal oxygen atoms (O2) of the $MO_5$ caps and the five coordinate M2 and M1′ atoms in the ring and on the other cap, respectively. As detailed above, the geometry optimization leads to a significant reduction in the length of the M2−O2 and M1′−O2 bonds. The bond orders for both types of bonds are also significant. If the M1′−O2 bonds are considered as genuine bonds, then the topology of the isomer becomes equivalent to that of the ($\beta-\gamma$) isomer suggested as an intermediate by Klemperer and Shum.[9] If the M2−O2 bonds are also considered as genuine bonds, then the topology becomes that of the $\beta$-isomer.

Mulliken charges for all atoms are listed in Table 8. Mulliken charges are well-known to exhibit basis set dependence, and indeed, this dependence has been shown to be intimately related to that of the Mayer bond order.[52] Nonetheless, the Mulliken method is compatible with approaches based on linear combination of atomic orbitals. It yields valuable information about relative charges when a consistent basis set is used, as here. We have previously demonstrated that qualitatively similar values and trends in atomic charges are obtained for isopolyanions with Mulliken and other population methods.[29]

For all of the octamolybdates, the metal charges are in the range of 2.1−2.4 with slightly higher values for the Mo atoms located in capping groups. In all cases, the Mo s- and p-orbitals are largely unpopulated. As in other isopolyanions,[28−35] the metal−oxygen bonding almost exclusively involves d-orbital participation from the high oxidation state metal. The negative charge is distributed over all types of oxygen atoms and increases in magnitude with the coordination number.

Also included in Table 7 are the covalencies and full valencies of the oxygen atoms and the number of each type of oxygen in the octamolybdates. The covalency of an atom is the sum of the bond orders made by the atom and includes small contributions from interactions such as those between the oxygen atoms. The full valency is a combined measure of the covalent (covalency) and ionic (electrovalent) bonding based on the Mayer and Mulliken results.

Figure 8 shows the correlation between these valency indexes and the Mulliken charges for all of the oxygen atoms in the octamolybdates. There is a clear, inverse correlation between the covalency and the Mulliken charge. There is a fairly clear separation of the covalent indexes and Mulliken charges for the oxygen atoms according to their coordinate number. Terminally bonded oxygen atoms have the lowest negative charges and highest covalencies. Pseudoterminal and $\mu_2$ oxygen atoms have similar covalencies with the latter having slightly

**TABLE 7: Mulliken Charges, Covalencies, and Full Valencies of the Mo and O Atoms in the Isomers of $[Mo_8O_{26}]^{4-}$ from Calculations at the LDA Optimized Geometries**

| | type | | charge | type | | charge | covalency | full valency |
|---|---|---|---|---|---|---|---|---|
| α | $Mo_{4c}$ | M1 (×2) | 2.27 | $O_t$ | O1 (×2) | −0.77 | 2.01 | 2.27 |
| | $Mo_{6c}$ | M2 (×6) | 2.10 | | O3 (×12) | −0.70 | 2.07 | 2.29 |
| | | | | $O_{2c}$ | O4 (×6) | −0.92 | 1.82 | 2.21 |
| | | | | $O_{3c}$ | O2 (×6) | −0.95 | 1.80 | 2.21 |
| β | $Mo_{6c}$ | M1 (×2) | 2.42 | $O_t$ | O1 (×2) | −0.71 | 2.06 | 2.28 |
| | | M2 (×4) | 2.24 | | O2 (×4) | −0.73 | 2.02 | 2.26 |
| | | M3 (×2) | 2.19 | | O3 (×8) | −0.73 | 2.03 | 2.27 |
| | | | | $O_{2c}$ | O4 (×2) | −0.85 | 1.87 | 2.20 |
| | | | | | O5 (×4) | −0.95 | 1.79 | 2.20 |
| | | | | $O_{3c}$ | O6 (×4) | −1.05 | 1.65 | 2.16 |
| | | | | $O_{5c}$ | O7 (×2) | −1.17 | 1.48 | 2.13 |
| γ | $Mo_{5c}$ | M1 (×2) | 2.23 | $O_t$ | O1 (×4) | −0.75 | 2.01 | 2.26 |
| | $Mo_{6c}$ | M2 (×2) | 2.42 | | O5 (×2) | −0.74 | 2.04 | 2.28 |
| | | M3 (×2) | 2.21 | | O6 (×4) | −0.75 | 2.01 | 2.25 |
| | | M4 (×2) | 2.29 | | O7 (×4) | −0.72 | 1.80 | 2.26 |
| | | | | $O_{2c}$ | O2 (×2) | −0.94 | 1.79 | 2.19 |
| | | | | | O8 (×2) | −0.85 | 1.90 | 2.22 |
| | | | | | O9 (×2) | −0.94 | 1.80 | 2.20 |
| | | | | $O_{3c}$ | O3 (×2) | −1.09 | 1.58 | 2.13 |
| | | | | | O4 (×2) | −1.10 | 1.59 | 2.17 |
| | | | | $O_{4c}$ | O10 (×2) | −1.04 | 1.66 | 2.17 |
| δ | $Mo_{4c}$ | M1 (×2) | 2.37 | $O_t$ | O1 (×2) | −0.79 | 1.98 | 2.26 |
| | | M2 (×2) | 2.22 | | O2 (×4) | −0.77 | 2.00 | 2.26 |
| | $Mo_{6c}$ | M3 (×4) | 2.26 | | O6 (×8) | −0.72 | 2.04 | 2.27 |
| | | | | $O_{2c}$ | O3 (×4) | −0.93 | 1.83 | 2.21 |
| | | | | | O4 (×4) | −0.98 | 1.77 | 2.21 |
| | | | | | O7 (×2) | −0.94 | 1.80 | 2.20 |
| | | | | $O_{3c}$ | O5 (×2) | −1.09 | 1.63 | 2.17 |
| ϵ | $Mo_{5c}$ | M1 (×2) | 2.38 | $O_t$ | O1 (×4) | −0.77 | 2.01 | 2.27 |
| | | M2 (×4) | 2.27 | | O2 (×8) | −0.73 | 2.03 | 2.26 |
| | $Mo_{6c}$ | M3 (×2) | 2.26 | | O7 (×4) | −0.74 | 2.02 | 2.27 |
| | | | | $O_{2c}$ | O4 (×4) | −0.94 | 1.80 | 2.20 |
| | | | | $O_{3c}$ | O5 (×4) | −1.07 | 1.61 | 2.14 |
| | | | | | O6 (×2) | −1.08 | 1.62 | 2.15 |
| ξ | $Mo_{5c}$ | M1 (×2) | 2.22 | $O_t$ | O1 (×4) | −0.74 | 2.02 | 2.26 |
| | | M2 (×2) | 2.23 | | O2 (×4) | −0.76 | 2.01 | 2.26 |
| | $Mo_{6c}$ | M3 (×2) | 2.40 | | O8 (×2) | −0.74 | 2.04 | 2.28 |
| | | M4 (×2) | 2.30 | | O9 (×4) | −0.72 | 2.03 | 2.27 |
| | | | | $O_{2c}$ | O3 (×2) | −0.94 | 1.79 | 2.20 |
| | | | | | O4 (×2) | −0.94 | 1.81 | 2.20 |
| | | | | | O10 (×2) | −0.85 | 1.91 | 2.23 |
| | | | | $O_{3c}$ | O5 (×2) | −1.06 | 1.61 | 2.14 |
| | | | | | O6 (×2) | −1.11 | 1.59 | 2.16 |
| | | | | | O7 (×2) | −1.08 | 1.62 | 2.16 |

higher charges. The high coordinate ($\mu_3$, $\mu_4$, and $\mu_5$) sites have the highest charges and significantly lower covalencies.

The full valency, however, varies to a much smaller extent, with a value of $2.2 \pm 0.1$ for all oxygen atoms irrespective of the isomer, coordination number, or local geometry. Indeed, although the Mulliken and Mayer values vary with basis set, the value of the full valency is fairly independent of the size of a balanced basis set. The apparent requirement of the oxygen atoms to achieve this valency irrespective of the coordination number suggested by the analysis of the electronic structure is, of course, fully consistent with classical views of valency.[53] It leads to important limitations and requirements on the structures of polyoxoanions.

A clear structural feature in polyoxoanions is the presence of long M−O bonds in trans configuration with respect to terminal groups. These long bonds are often described[2] as a manifestation of the strong trans influence of multiply bonded oxo sites. This feature is illustrated by a number of bonds in the octamolybdates including the M2−O10 and M3−O3 bonds in the γ-form, the M3−O5 bond in the δ-form, the M3−O5 bond in the ϵ-form, and the M3−O6 and M3−O7′ bonds in the ξ-form, as well as the apparently facile interconversion between distorted octahedral and square pyramidal coordination evident in these structures. Although the Mayer bond orders for these bonds suggest that they are individually rather weak, the oxygen atoms involved are not, as has been pointed out by Tytko et al.,[51] weakly bound sites. The full valency indexes for these oxygen atoms are comparable with other sites. The oxygen atoms that are affected by trans influence effects counterbalance the weakened bond by adopting high-coordination environments. As the vertexes on the surface of polyoxoanions are terminal oxygen sites, the structural requirement for the trans-located oxygen atoms to be high coordination sites leads to the adoption of clusters and capped rings of the type displayed by the octamolybdates.

**Bonding Energetics.** The relative energies of the isomers are listed in Table 7. The energies correspond to single point BP86 calculations at the crystallographic (expt) and LDA-optimized (calcd) geometries. In all cases, the energy of the optimized structure lies significantly below that of the crystal structure. The calculations suggest that the α- and δ-isomers are the most intrinsically stable in the absence of a general or specific stabilization from the environment. The β-isomer, although a major component of aqueous solutions containing Mo(VI) at pH 2, is actually calculated to be the least stable of the known isomeric forms both in its crystallographically determined and optimized geometries. As the isomers all have the same charge and approximate size, its occurrence is presumably due to specific coordination, by solvent or counterion, or is kinetic in origin. Previously reported calculations[35] using the hybrid functional B3LYP suggest an even larger energy difference between the α- and the β-forms.

Further insight into the energy differences between the isomers can be afforded if the molecular bonding or atomization energy ($E_B$) is decomposed as

$$E_B = E_O + E_P + E_E$$

where $E_O$, $E_P$, and $E_E$ represent orbital mixing, Pauli repulsion, and electrostatic interaction terms, respectively. Descriptions of the physical significance of these properties have been given by Landrum, Goldberg and Hoffmann,[54] and Baerends and coworkers.[43,55] Both $E_O$ and $E_P$ arise from orbital interaction effects with the former stabilizing and the latter destabilizing. $E_O$ represents the effect of charge transfer, orbital mixing, and polarization when filled and empty atomic orbitals overlap. The $E_P$ component is obtained by the requirement of antisymmetry and can be considered as the effect of the interaction between filled orbitals. The resulting destabilization, labeled as Pauli, exchange, or overlap repulsion, has been described as a measure of steric interaction. The $E_E$ contribution arises from the Coulombic interaction between the atoms, before any orbital relaxation occurs. It is dominated by nucleus−electron attractions.

Table 8 shows the decomposition of the bonding energy for the octamolybdate isomers corresponding to single point BP86 calculations at the crystallographic and LDA optimized geometries. The values and trends in the energetic terms can be related to the structures and to the bond order indexes described above.

As discussed above, the trans influence of the terminal oxo groups lying on the surface of polyoxoanions leads to the requirement that the trans-located oxygen atoms adopt sites of high coordination number. This requirement, on its own, leads to compact shapes with the trans-located oxygen atoms shared between a number of $MO_x$ polyhedra. The β-isomer exhibits the most compact and most nearly spherical structure of the

**TABLE 8: Bonding Energetics (in eV) and Relative Energies (in kJ mol$^{-1}$) of the Isomers of $[Mo_8O_{26}]^{4-}$ from Single Point BP86 Calculations at the Crystallographic (expt) and LDA Optimized (calcd) Geometries**

| | | $E_O$ | $E_E$ | $E_P$ | $E_B$ | $\Delta_{rel}$ |
|---|---|---|---|---|---|---|
| α | expt | −679.03 | −225.72 | +633.24 | −271.52 | +99 |
| | calcd | −656.72 | −215.19 | +599.39 | −272.52 | +4 |
| *β* | expt | −677.77 | −229.22 | +636.29 | −270.70 | +178 |
| | calcd | −662.34 | −221.41 | +612.28 | −271.48 | +112 |
| *γ* | expt | −677.92 | −227.76 | +634.49 | −271.19 | +130 |
| | calcd | −657.77 | −217.39 | +602.84 | −272.32 | +21 |
| *δ* | expt | −679.04 | −226.02 | +633.67 | −271.39 | +111 |
| | calcd | −654.24 | −213.56 | +595.27 | −272.54 | 0 |
| *ϵ* | expt | −676.08 | −226.99 | +632.01 | −271.06 | +142 |
| | calcd | −660.71 | −219.74 | +608.55 | −271.90 | +62 |
| *ξ* | expt | −677.02 | −228.03 | +634.26 | −270.80 | +168 |
| | calcd | −657.39 | −217.26 | +602.42 | −272.22 | +31 |

known octamolybdates. However, it is predicted to be the least intrinsically stable of the octamolybdates studied here. The decomposition of the bonding energy shows that this originates in the destabilizing $E_P$ term, which is considerably higher for the *β*-isomer than for the other forms. The compact nature of the packing in the *β*-isomer leads to it having the greatest number of Mo−O bonds (48), and this leads to it being the most sterically crowded, as measured by $E_P$.

The value of $E_P$ for the octamolybdates correlates very well with the number of Mo−O bonds making up the structure, with the apparent exception of the *ϵ*-isomer. This structure contains only 42 Mo−O bonds but has a relatively high $E_P$. This bond count, however, is based on the O2 atoms being labeled as terminal groups. The structural and bond order analysis described above suggests that there is some degree of bonding between O2 and the five coordinate metal sites M1′ and M2. If these interactions are included, the $E_P$ value is not exceptional. The *δ*-isomer, calculated to be the most intrinsically stable form, has the fewest bonds (40) and so the least destabilizing $E_P$ term.

The orbital interaction and electrostatic terms in the bond energy also correlate with the number of Mo−O bonds. More compact structures should lead to more extensive overlap of orbitals and charge distributions. Thus, the optimized structure of the *β*-form has the most stabilizing values for both $E_O$ and $E_E$. The optimized structure of the *δ*-isomer has the least stabilizing $E_O$ and $E_E$ values, consistent with it having the fewest Mo−O bonds.

The stability of different isomeric forms of polyoxoanions appears to be a balance between minimizing steric crowding ($E_P$), through the adoption of more open structures with small numbers of high coordinate oxygen atoms, and the demands of oxygen valency ($E_O$ and $E_E$), requiring higher coordination numbers for oxygen atoms located trans to terminal Mo−O bonds. The relatively small energy differences between the octamolybdate isomers arise directly from this balance.

## Conclusion

The molecular and electronic structure of the α-, *β*-, *γ*-, *δ*-, *ϵ*-, and *ξ*-isomers of $[Mo_8O_{26}]^{4-}$ isopolyanions have been calculated using DF theory. The structures of the *γ*-, *δ*-, *ϵ*-, and *ξ*-isomers have been optimized at the LDA level, complementing our earlier study of the α- and *β*-forms. The optimized structures are in reasonably good agreement with those determined experimentally with the exception of the *γ*-form. For this isomer, the optimization leads to a lengthening of an internal bond with a resulting decrease in coordination number from six to five for one of the metal atoms. As a result, the topology of this isomer becomes identical to that of the *ξ*-form.

A bond order and valency analysis of the isomers has been reported. The Mo−O bond order decreases exponentially with bond length. The terminal Mo−O bonds possess fractional multiple bond character with similar values for those attached to four, five, and six coordinate metal atoms. The Mo−O bond order decreases as the coordination number of the oxygen increases, and a number of pseudoterminal oxygen sites have been located. These oxygen atoms formally bridge two metal sites but are involved in one strong and one weak bond. The weak bond, however, must still be considered a genuine interaction. The bond order analysis appears to confirm the coordination numbers of the metal atoms in the *δ*- and *ξ*-isomers despite reasonably close contacts with additional oxygen atoms. The analysis suggests, however, that additional contacts should be considered for one of the terminal atoms in the $MO_5$ capping groups of the *ϵ*-isomer leading to a topology intermediate between that of the *β*-isomers and of the previously predicted (*β*−*γ*) intermediate. The charge on the metal atoms is reasonably similar in all of the isomers, with slightly higher charges being found for those involved in capping groups. As observed in previous analyses, the metal−oxygen bonding is predominately between metal d-orbitals and oxygen p-orbitals. The negative charge in the clusters is distributed over all oxygen sites and is predicted to increase with the coordination number of the oxygen. Despite the range of coordination numbers, charges, and bond orders, the overall bonding capacity of the oxygen atoms, measured through the full valency index, appears similar. Mo−O bonds located trans to terminal oxo groups suffer a large trans influence leading to weak bonds with low bond orders. The oxygen atoms achieve their full valence by adopting high coordination numbers leading to restrictions on the possible polyoxoanion geometries.

The α- and *δ*-isomers are predicted to be the most intrinsically stable while the *β*-form is the least stable. A decomposition of the bonding energy suggests that the compact structure of the *β*-form leads to highly unfavorable steric interactions and favorable orbital and electrostatic interactions between the atoms. The apparent relative instability of this isomer is due to its sterically crowded structure. The contributions from steric crowding and favorable atomic interactions correlate with the number of Mo−O bonds, and the balance between them leads to relatively small energy differences between the other isomers.

**Acknowledgment.** We thank EPSRC and the University of Hull for financial support and the U.K. Computational Chemistry Working Party for access to computational facilities in the Rutherford Appleton Laboratory.

## References and Notes

(1) Pope, M. T. *Heteropoly and Isopoly Oxometalates*; Springer-Verlag: Heidelberg, 1983.
(2) Pope, M. T.; Müller, A. *Angew. Chem., Int. Ed. Engl.* **1991**, *30*, 34.
(3) Baker, L. C. W.; Glick, D. C. *Chem. Rev.* **1998**, *98*, 3.
(4) Pope, M. T., Müller, A. *Polyoxometalates: from Platonic Solids to Anti-Retroviral Activity*; Kluwer: Dordrecht, 1994.
(5) Schwing-Weill, M. J.; Arnaud-Neu, F. *Bull. Soc. Chim. Fr.* **1970**, 853.
(6) Fuchs, J.; Hartl, H. *Angew. Chem., Int. Ed. Engl.* **1976**, *15*, 375.
(7) (a) Lindqvist, I. *Ark. Kemi* **1950**, *2*, 349. (b) Atovmyan, L. O.; Krasochka, O. N. *J. Struct. Chem.* **1972**, *13*, 319.
(8) Himeno, S.; Niiya, H.; Ueda, T. *Bull. Chem. Soc. Jpn.* **1997**, *70*, 631.
(9) Klemperer, W. G.; Shum, W. *J. Am. Chem. Soc.* **1976**, *98*, 8291.
(10) Niven, M. L.; Cruywagen, J. J.; Heyns, J. B. B. *J. Chem. Soc., Dalton Trans.* **1991**, 2007.
(11) Hagrman, D.; Zubieta, C.; Hauschalter, R. C.; Zubieta, J. *Angew. Chem., Int. Ed. Engl.* **1997**, *36*, 873.

(12) Hagrman, D.; Hagrman, P.; Zubieta, J. *Inorg. Chim. Acta* **2000**, *300*, 212.
(13) Rarig, R. S., Jr.; Zubieta, J. *Inorg. Chim. Acta* **2001**, *312*, 188.
(14) Xi, R.; Wang, B.; Isobe, K.; Nishioka, T.; Toriumi, K.; Ozawa, Y. *Inorg. Chem.* **1994**, *33*, 833.
(15) Xu, J.-Q.; Wang, R.-Z.; Yang, G.-Y.; Xing, Y.-H.; Li, D.-M.; Bu, W.-M.; Ye, L.; Fan, Y.-G.; Yang, G.-D.; Xing, Y.; Lin, Y.-H.; Jia, H.-Q. *Chem. Commun.* **1999**, 983.
(16) Rohmer, M.-M.; Ernenwein, R.; Ulmschneider, M.; Wiest, R.; Bénard, M. *Int. J. Quantum Chem.* **1991**, *40*, 723.
(17) Kempf, J.-Y.; Rohmer, M.-M.; Poblet, J.-M.; Bo, C.; Bénard, M. *J. Am. Chem. Soc.* **1992**, *114*, 1136.
(18) Rohmer, M.-M.; Bénard, M. *J. Am. Chem. Soc.* **1994**, *116*, 6959.
(19) Devémy, J.; Rohmer, M.-M.; Bénard, M.; Ernenwein, R. *Int. J. Quantum Chem.* **1996**, *58*, 267.
(20) Rohmer, M.-M.; Devémy, J.; Wiest, R.; Bénard, M. *J. Am. Chem. Soc.* **1996**, *118*, 13007.
(21) Maestre, J. M.; Sarasa, J. P.; Bo, C.; Poblet, J. M. *Inorg. Chem.* **1998**, *37*, 3071.
(22) Maestre, J. M.; Poblet, J. M.; Bo, C.; Casañ-Pastor, N.; Gomez-Romero, P. *Inorg. Chem.* **1998**, *37*, 3444.
(23) Dolbecq, A.; Guirauden, A.; Fourmigué, M.; Boubekeur, K.; Batail, P.; Rohmer, M.-M.; Bénard, M.; Coulon, C.; Sallé, M.; Blanchard, P. *J. Chem. Soc., Dalton Trans.* **1999**, 1241.
(24) Maestre, J. M.; López, X.; Bo, C.; Poblet, J. M.; Casañ-Pastor, N. *J. Am. Chem. Soc.* **2001**, *23*, 3749.
(25) Rohmer, M.-M.; Bénard, M.; Blaudeau, J.-P.; Maestre, J. M.; Poblet, J. M. *Coord. Chem. Rev.* **1998**, *178*, 1019.
(26) López, X.; Maestre, J. M.; Poblet, J. M.; Bo, C. *J. Am. Chem. Soc.* **2001**, *123*, 9571.
(27) Maestre, J. M.; Lopez, X.; Bo, C.; Poblet, J.-M. *Inorg. Chem.* **2002**, *41*, 1883.
(28) Bridgeman, A. J.; Cavigliasso, G. *Polyhedron* **2001**, *20*, 2269.
(29) Bridgeman, A. J.; Cavigliasso, G. *J. Phys. Chem. A* **2001**, *105*, 7111.
(30) Bridgeman, A. J.; Cavigliasso, G. *Polyhedron* **2001**, *20*, 310.
(31) Bridgeman, A. J.; Cavigliasso, G. *J. Chem. Soc., Dalton Trans.* **2001**, 3556.
(32) Bridgeman, A. J.; Cavigliasso, G. *Inorg. Chem.* **2002**, *41*, 1761.
(33) Bridgeman, A. J.; Cavigliasso, G. *J. Chem. Soc., Dalton Trans.* **2002**, 2244.
(34) Bridgeman, A. J.; Cavigliasso, G. *J. Phys. Chem. A* **2002**, *106*, 6114.
(35) Bridgeman, A. J.; Cavigliasso, G. *Inorg. Chem.* **2002**, *41*, 3500.
(36) Bridgeman, A. J.; Cavigliasso, G. Submitted for publication.
(37) Bridgeman, A. J.; Cavigliasso, G. *Chem. Phys.* **2002**, *279*, 143.
(38) Duclusaud, H.; Borshch, S. A. *Inorg. Chem.* **1999**, *38*, 3489.
(39) Duclusaud, H.; Borshch, S. A. *J. Am. Chem. Soc.* **2001**, *123*, 2835.
(40) Borshch, S. A.; Duclusaud, H.; Millet, J. M. M. *Appl. Catal. A* **2000**, *200*, 103.
(41) Nomiya, K.; Miwa, M. *Polyhedron* **1984**, *3*, 341.
(42) (a) ADF2000.02; Baerends, E. J.; Ellis, D. E.; Ros, P. *Chem. Phys.* **1973**, *2*, 41. (b) Versluis, L.; Ziegler, T. *J. Chem. Phys.* **1988**, *88*, 322. (c) te Velde, G.; Baerends, E. J. *J. Comput. Phys.* **1992**, *99*, 84. (d) Fonseca Guerra, C.; Snijders, J. G.; te Velde, G.; Baerends, E. J. *Theor. Chem. Acc.* **1998**, *99*, 391.
(43) te Velde, G.; Bickelhaupt, F. M.; Baerends, E. J.; Fonseca Guerra, G.; Snijders, J. C.; Ziegler, T. *J. Comput. Chem.* **2001**, *22*, 931.
(44) Vosko, S. H.; Wilk, L.; Nusair, M. *Can. J. Phys.* **1980**, *58*, 1200.
(45) Kohn, W.; Sham, L. J. *Phys. Rev. A* **1965**, *140*, 1133.
(46) Becke, A. D. *Phys. Rev. A* **1988**, *38*, 3098.
(47) Perdew, J. P. *Phys. Rev. B* **1986**, *33*, 8822.
(48) (a) Mayer, I. *Chem. Phys. Lett.* **1983**, *97*, 270. (b) Mayer, I. *Int. J. Quantum Chem.* **1984**, *26*, 151.
(49) Evarestov, R. A.; Veryazov, V. A. *Theor. Chim. Acta* **1991**, *81*, 95.
(50) Bridgeman, A. J. *MAYER*; a program to calculate Mayer bond-order indexes from the output of the electronic structure packages GAMESS-UK, Gaussian 98 and ADF; University of Hull: Hull, U.K., 2001. Available from the author on request.
(51) Tytko, K. H.; Mehmke, J.; Fischer, S. *Struct. Bonding (Berlin)* **1999**, *93*, 129.
(52) Bridgeman, A. J.; Cavigliasso, G.; Ireland, L. R.; Rothery, J. *J. Chem. Soc., Dalton Trans.* **2001**, 2095.
(53) Pauling, L. *The Nature of the Chemical Bond*; Cornell University Press: New York, 1960.
(54) Landrum, G. A.; Goldberg, N.; Hoffman, R. *J. Chem. Soc., Dalton Trans.* **1997**, 3605.
(55) Bickelhaupt, F. M.; Baerends, E. J. *Rev. Comput. Chem.* **2000**, *15*, 1.